Attosecond time delay spectroscopy of the hydrogen molecule

I. A. Ivanov* and A. S. Kheifets
Research School of Physical Sciences, The Australian National University, Canberra ACT 0200, Australia

Vladislav V. Serov
Department of Theoretical Physics, Saratov State University, 83 Astrakhanskaya, Saratov 410012, Russia
(Dated: July 4, 2012)

We apply the concept of photoemission time delay to the process of single-photon one-electron ionization of the H_2 molecule. We demonstrate that, by resolving the photoelectron detection in time on the attosecond scale, one can extract differential photoionization cross sections for particular field/molecule orientations from the measurement on a randomly oriented molecule

PACS numbers: 32.80.Rm 32.80.Fb 42.50.Hz

Attosecond science has extended experimental studies of atomic and molecular photoionization into a new dimension. In atoms, a time delay between absorption of an attosecond XUV pulse and subsequent emission of a photoelectron has been measured [1, 2, 3]. In molecules, electron localization and attosecond control have been demonstrated in pump-probe photoionization experiments [4, 5]. Experimental time-delay studies in molecules are yet to be performed either by using the attosecond streaking [1] or by the interferometric sideband oscillation technique [2]. In the meantime, molecules offer a very rich and complex photoionization picture in which the cross-section and angular distribution of photoelectrons depend sensitively on the molecular orientation relative to the polarization axis of VUV radiation. Thus the attosecond time delay studies can be very beneficial to molecular photoionization by defining the phase of the ionization amplitude and thus achieving the complete photoionization experiment [6].

In the simplest case of a homonuclear diatomic molecule, its orientation is defined by the mutual angle θ_N of the molecular and polarization axes. Photoionization cross-section and angular distribution of photoelectrons in H_2 and D_2 depend strongly on this angle varying between the limits of Σ ($\theta_N = 0$) and Π ($\theta_N = 90^\circ$) orientations. In single photoionization, the amplitude and cross-section of the Σ orientated H_2 display a deep minimum [7] which can be attributed to the two-center electron interference [8]. In double photoionization (DPI), the angular correlation pattern in two-electron continuum shows strong variation with the angle θ_N. Because of the Coulomb explosion of the doubly ionized H_2 molecule, its orientation at the moment of ionization can be measured experimentally [9, 10]. In principle, neutral polarizable molecules can also be aligned by a strong laser field [11]. However, reports of single photoionization of aligned molecules are not known to the authors.

In this Letter, we offer an alternative strategy of attosecond studies of randomly oriented molecules. Within the framework of the time delay theory [12, 13] and by employing the saddle-point method, we figure out that the phase of the electron wave packet, emanated from the randomly oriented molecule, carries information about the angle differential photoionization cross-section specific to certain molecular orientations. By extracting this information, one can effectively measure the orientation specific cross-sections without actually aligning the molecule. In the following, we illustrate our findings by using a process of single-photon one-electron ionization of the H_2 molecule as a convenient example.

We shall be interested in the probability density distribution $P(t)$ to detect an electron at the moment of time t using a detector placed at a point $\boldsymbol{r}$ far away from the ionized molecule. The time-dependent wave function of the ejected electron after the end of the laser pulse can be written as

$$\Psi(\boldsymbol{r},t)=\int d\boldsymbol{q} f(\boldsymbol{q})\Psi^-_{\boldsymbol{q}}(\boldsymbol{r})e^{-iEt} \ , \qquad (1)$$

where $\Psi^-_{\boldsymbol{q}}(\boldsymbol{r})$ are the (ingoing) scattering states in the field of the molecular ion and $f(\boldsymbol{q})$ is the photoionization amplitude. A complete expansion of the wave function should include bound states as well but they do not propagate to large distances and hence do not affect the asymptotic behavior of the wave packet, so we omit them. For large t and r, the integral in Eq. (1) can be evaluated using the saddle-point method. For the wavepacket, describing an electron escaping with the asymptotic momentum $\boldsymbol{k}$, the amplitude $|f(\boldsymbol{q})|$ in Eq. (1) can be represented near its maximum as $f(\boldsymbol{q}) \simeq \exp[-a(q_{||}-k)^2 + i\delta(\boldsymbol{q}) - bq_\perp^2]$, where $\boldsymbol{q}_{||}$ and $\boldsymbol{q}_\perp$ are the components of the vector $\boldsymbol{q}$ in the direction of asymptotic momentum $\boldsymbol{k}$ and perpendicular direction, respectively. The quantity $\delta(\boldsymbol{q})$ is the phase of the ionization amplitude. The parameter b characterizes the spread of the wavepacket in the lateral direction, and it is determined ultimately by the experimental geometry. The parameter a characterizes the spread of the wavepacket in the direction of the momentum vector $\boldsymbol{k}$ towards the detector. If the wavepacket is well collimated and the parameter b is large, so that $b \gg a$, then the energy spread of the

*Electronic address: Igor.Ivanov@anu.edu.au

wavepacket is approximately $\Delta E \approx k/\sqrt{a}$ which, in turn, is equal approximately to the bandwidth of the driving laser pulse.

The large t asymptotic behavior of the wave function (1) is determined by the $q_{||}$ integration. The scattering states in Eq. (1) are asymptotically Coulomb waves $\Psi^-_{\boldsymbol{q}} \propto e^{i\boldsymbol{q}\boldsymbol{r}+i\gamma(\boldsymbol{r},\boldsymbol{q})}$ with $\gamma(\boldsymbol{r},\boldsymbol{q}) = q^{-1}\ln(rq+\boldsymbol{r}\boldsymbol{q})$ [1, 15, 16]. Therefore the saddle point, that determines the large t behavior of the integral in Eq. (1), is a critical point of the expression

$$S(\boldsymbol{q}_{||},t) = -a(q_{||}-k)^2 + i\delta(q_{||}) - iq_{||}^2 t/2 + i\boldsymbol{q}_{||}\boldsymbol{r} + i\gamma(\boldsymbol{r},\boldsymbol{q}_{||}) \ . \tag{2}$$

This critical point determines the asymptotic electron trajectory

$$\boldsymbol{r}(t) \asymp \boldsymbol{k}(t-t_0) + \boldsymbol{r}'(t) \ . \tag{3}$$

Here $t_0(E) = k^{-1}d\delta/dq_{||}$ is the time delay and $\boldsymbol{r}'(t) = -d\gamma(\boldsymbol{r},\boldsymbol{q}_{||})/d\boldsymbol{q}_{||}$ is a known function varying logarithmically slow with t. All the derivatives here are assumed to be taken at the point $\boldsymbol{q}_{||} = \boldsymbol{k}$.

To find the probability of the electron detection as a function of time, we have to evaluate the integral in Eq. (1). By using the saddle-point method, expanding Eq. (2) around the critical point and retaining the quadratic terms, we arrive at the following expression:

$$\Psi(\boldsymbol{r},t) \propto \exp\left\{-\frac{[\boldsymbol{r}-\boldsymbol{k}(t-t_0)-\boldsymbol{r}'(t)]^2}{4a}\right\} \tag{4}$$

The squared modulus of the wave function (4) defines the probability $P(t,\boldsymbol{R},\theta_N)$ for an electron to arrive at the moment of time t at the detector placed at the point $\boldsymbol{R} = \boldsymbol{n}R$

$$P(t,\boldsymbol{R},\theta_N) = A(\boldsymbol{n},\theta_N)\exp\left\{-\frac{k^2[t-t_0(\boldsymbol{n},\theta_N)-\tau]^2}{2a}\right\} \ . \tag{5}$$

Here we introduced the arrival time τ defined as a root of the equation:

$$\boldsymbol{R} = \boldsymbol{k}\tau + \boldsymbol{r}'(\tau). \tag{6}$$

From Eq. (6) and the definition of the function $\boldsymbol{r}'(t)$ above, it is clear that the arrival time depends only on the experimental geometry and does not depend on the field/molecule orientation. The physical meaning of the arrival time is obvious. It corresponds to the moment of time at which the distribution of the electrons, arriving at the detector, as a function of time would have peaked in the absence of any time delay. When deriving Eq. (5), we also took account of the fact that both the pre-exponential factor and the time delay t_0 depend on the unit vector $\boldsymbol{n} = \boldsymbol{R}/R$ in the direction of the detector and the mutual field/molecule orientation, defined by the angle θ_N. The pre-exponential factor can be found by noting that the integration of $P(t,\boldsymbol{R},\theta_N)$ over time should give us the total probability to detect an electron escaping in a given direction. The latter can be expressed in terms of the differential cross-section and the total energy carried by the laser pulse [14]. For the coefficient in Eq. (5) we thus obtain:

$$A(\boldsymbol{n},\theta_N) = \frac{k_0 c}{8\pi^{\frac{3}{2}}\omega}\frac{d\sigma(\boldsymbol{n},\theta_N)}{d\Omega}\int F^2(t)\ dt \ . \tag{7}$$

Here $c \approx 137$ is the speed of light in atomic units. The integral of the squared electric field intensity $F(t)$ is taken over the duration of the pulse. This integral is related to the total energy of the laser pulse which is usually known in the experiment. The signal measured at the detector is an average over all possible molecular orientations:

$$P_{\rm av}(t) = \int_0^{\frac{\pi}{2}} P(t,\theta_N)\sin\theta_N\ d\theta_N \tag{8}$$

As a numerical example, we consider here the process of single-photon one-electron ionization of H_2 for the photon energy $\omega = 64$ eV. We consider the geometry in which photoelectrons are detected in the z direction of the polarization vector of the laser field. Numerical data, that are required to evaluate Eqs. (5) and (8), are computed using the exterior complex scaling method in prolate spheroidal coordinates (PSECS) [17]. These data are the angle differential cross-section in the direction of the photoelectron detection and the time delay corresponding to the given photoelectron energy E. The latter is computed as

$$t_0(\boldsymbol{n},\theta_N) = {\rm Im}\left[\frac{df(\boldsymbol{n},\theta_N)}{dE}\frac{1}{f(\boldsymbol{n},\theta_N)}\right] \ , \tag{9}$$

where $f(\boldsymbol{n},\theta_N)$ is the photoionization amplitude. The energy derivative is evaluated using the finite difference formula by running PSECS calculations for two closely spaced energies. For the parameter a in Eq. (5) we used the value $a = 20$ a.u. which gives us the characteristic spread of the electron wavepacket of 10 eV. With the carrier frequency of 64 eV, this corresponds to a rather short pulse. We emphasize that the exact shape of this pulse (Gaussian or not) is not relevant to our analysis. All we need for the saddle point derivation is a quadratic expansion of the modulus of the ionization amplitude near the critical point, which is always valid.

Our numerical results are presented on the top panel of Fig. 1 in the form of the photoelectron detection probability distribution $P_{\rm av}(t)$ as a function of time measured from the moment of arrival τ. On the same panel, we also display the probability distribution $P^0_{\rm av}(t)$, obtained if in Eq. (5) we put time delays to zero. The difference between the time delayed and zero delayed probabilities is highlighted on the bottom panel of Fig. 1 where we display the normalized difference signal $[P_{\rm av}(t) - P^0_{\rm av}(t)]/P^0_{\rm av}(t)$. As can be seen from Eq. (5) and Fig. 1, the probability $P^0_{\rm av}(t)$ is an even function of $t = \tau$ peaked at $t - \tau = 0$. The time delays $t_0(\boldsymbol{n},\theta_N)$,

which are different for different orientations θ_N, are responsible for the asymmetry of the averaged distribution visible on both panels of Fig. 1.

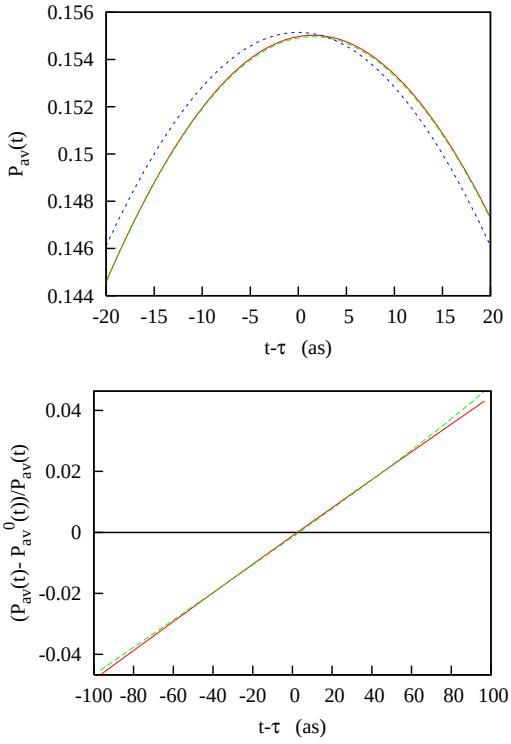

FIG. 1: (Color online) Top panel: The angular averaged probability distribution $P_{\rm av}(t)$ computed according to Eqs. (5) and (8) is shown by the solid (red) line. The dash (green) line: results of the fitting procedure. The (blue) dots: distribution $P^0_{\rm av}(t)$ computed assuming zero time delays in Eq. (5). Bottom panel: The normalized difference signal $[P_{\rm av}(t) - P^0_{\rm av}(t)]/P^0_{\rm av}(t)$.

The computational procedure, that we described above, solves the direct problem of evaluating the probability distribution of the counts on the detector as a function of time. Now we demonstrate that the inverse problem can also be solved, i.e. one can extract information about the cross-sections and time delays for particular values of field/molecule orientation using the averaged signal $P_{\rm av}(t)$. The amplitude $f(\theta_N)$ and its energy derivative can be parametrized as functions of the angle θ_N [18]

$$\begin{aligned} f(\theta_N) &= \beta_1 \cos\theta_N + \beta_2 \sin\theta_N \\ \frac{df(\theta_N)}{dE} &= \beta_3 \cos\theta_N + \beta_4 \sin\theta_N \ , \end{aligned} \qquad (10)$$

where β_i are some complex parameters. With these parameters, we can find the differential cross section and the time delay entering Eqs. (5) and (7) (for the time delay we use Eq. (9)). The parameter a, which describes the momentum distribution of the electrons near the crest of the wave packet, is rarely, if ever, known in the experiment. We treat it, therefore, as an additional fitting parameter. This gives us a set of fitting parameters $\boldsymbol{\beta}, a$. With this set of parameters, we compute the trial distribution $P_{\rm trial}(t)$ using Eqs. (5), (8) and (10). With $P_{\rm trial}(t)$ thus computed, and $P_{\rm av}(t)$ presumed to be known, we form a functional

$$d(\boldsymbol{\beta}, a) = \int_{-\infty}^{\infty} \left[P_{\rm trial}(t) - P_{\rm av}(t)\right]^2 \ dt \qquad (11)$$

By minimizing $d(\boldsymbol{\beta}, a)$ with respect to the fitting parameters, we find the amplitude as a function of the angle θ_N. The result of such a fit for the probability distribution is shown in Fig. 1 for the photon energy $\omega = 64$ eV. The fitted curve is almost indistinguishable from the original calculation.

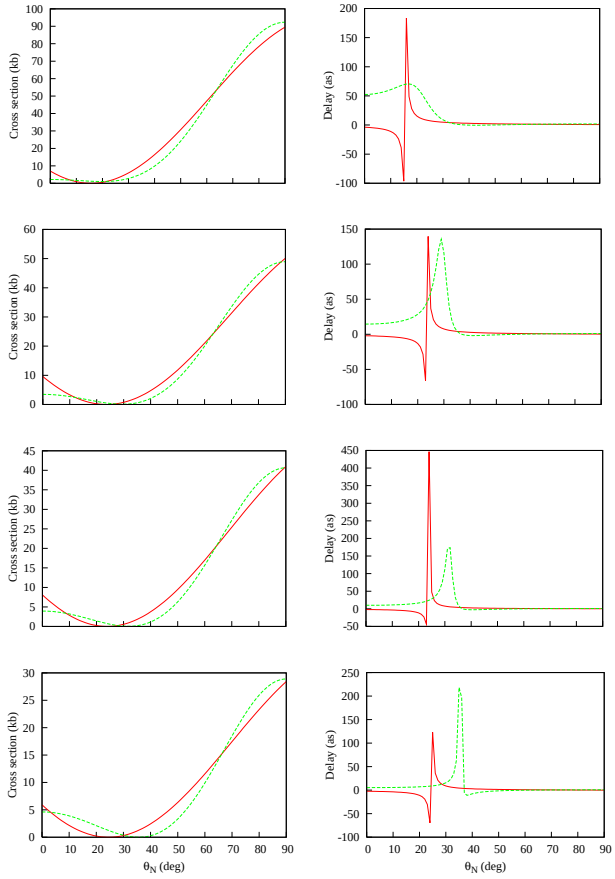

FIG. 2: (Color online) Differential cross sections of detecting the photoelectron in the z direction (left column) and corresponding time delays (right column) as functions of angle between molecular axis and field direction for photon energies of 64 eV (first row), 79 eV (second row), 84 eV (third row), and 94 eV (lower row). Solid (red) line- data obtained using the fitting procedure, dash (green)- calculated results.

By knowing the optimal set of fitting parameters $\boldsymbol{\beta}$, we can compute the cross section and the time delay as functions of the angle θ_N. These results are shown in Fig. 2 for four fixed photon energies $\omega = 64$, 79, 84 and 94 eV

along with the original data computed by the PSECS method. One can see that our fitting procedure reproduces the PSECS cross-section data quite reasonably except for the angles θ_N where this cross-section becomes small. That could be expected as the pre-exponential factor in Eq. (5) dampens heavily the probability making the fitting procedure insensitive to the contribution from these angles. Since the time delay is generally large when the cross section is small, the agreement of the fitted and exact time delays in Fig. 2 is not nearly as good as for the cross sections.

The interval of the photon energies that we considered includes the deep minimum at approximately 75 eV for the Σ orientation. The ratio of the cross sections σ_Π/σ_Σ shows a prominent maximum at this photon energy [7], where it is approximately an order of magnitude larger than for the photon energies far from the minimum. This means that, for the photon energies near 75 eV, the cross section as a function of the angle θ_N varies much more on the interval $\theta_N \in (0, \pi/2)$ than for the photon energies away from the minimum. Reproducing correctly a widely varying function using a fitting procedure is a more difficult task, than reproducing a function which is nearly constant. We have, therefore, tested our procedure for the most challenging interval of the photon energies.

To summarize, we described a procedure that allows one to extract information about the differential cross sections for particular field/molecule orientations from the measurement, on a randomly oriented molecule, of the probability to detect a photoelectron resolved in time. To do so, as one can see from Fig. 1, the resolution of the detector should be of the order of 10 as. This resolution cannot be achieved at present in XUV pump-probe experiments. However, one can employ the attoseecond streaking technique by using the ionizing XUV pump and a streaking infrared (IR) probe [19, 20]. This technique converts short intervals of time of the oreder of several attoseconds into more easily measurable physical characteristics such as photoelectron spectra. It is by using this technique that one can measure attosecond intervals of time such as the time delay between photo-electrons emitted from different shells [1], or the characteristic time an electron takes to tunnel out in the photo-ionization event [21, 22].

Authors are grateful to Misha Ivanov for valuable discussions. IAI and ASK acknowledge support of the Australian Research Council in the form of the Discovery grant DP0985136. VVS acknowledges support of the President of the Russian Federation (Grant No. MK-2344.2010.2) and the Russian Foundation for Basic Research (Grant No. 11-01-00523-a). Resources of the Australian National Computational Infrastructure Facility were used in this work.

[1] M. Schultze, et al., Science **328**(5986), 1658 (2010).
[2] K. Klünder, et al., Phys. Rev. Lett. **106**(14), 143002 (2011).
[3] D. Guénot, et al., Phys. Rev. A **85**, 053424 (2012).
[4] G. Sansone, et al., Nature **465**, 763 (2010).
[5] F. Kelkensberg, et al., Phys. Rev. Lett. **107**, 043002 (2011).
[6] U. Becker and A. Crowe, eds., *Complete Scattering Experiments*, Physics of Atoms and Molecules (Kluwer Academic Publishers, New York, 2002).
[7] S. K. Semenov and N. A. Cherepkov, J. Phys. B **36**(7), 1409 (2003).
[8] L. Nagy, S. Borbély, and K. Póra, Phys. Lett. A **327**(5-6), 481 (2004).
[9] T. Weber, et al., Phys. Rev. Lett. **92**(16), 163001 (2004).
[10] T. Weber, et al., Nature **431**(7007), 437 (2004).
[11] B. Friedrich and D. Herschbach, Phys. Rev. Lett. **74**, 4623 (1995).
[12] E. P. Wigner, Phys. Rev. **98**, 145 (1955).
[13] C. A. A. de Carvalho and H. M. Nussenzveig, Phys. Rep. **364**, 83 (2002).
[14] R.G.Newton, *Scattering theory of waves and particles* (McGraw-Hill, New York, 1966).
[15] A. S. Kheifets and I. A. Ivanov, Phys. Rev. Lett. **105**(23), 233002 (2010).
[16] I. A. Ivanov, Phys. Rev. A **83**(2), 023421 (2011).
[17] V. V. Serov and B. B. Joulakian, Phys. Rev. A **80**, 062713 (2009).
[18] J. M. Feagin, J. Phys. B **31**(18), L729 (1998).
[19] A. Baltuska *et al*, Nature **421**, 611 (2003).
[20] R. Kienberger, et al., Nature **427**, 817 (2004).
[21] P. Eckle, et al., Science **322**(5), 1525 (2008).
[22] D. Shafir, et al., Nature **485**, 343 (2012).